ELSEVIER

Journal of Nuclear Materials 313–316 (2003) 1211–1215

journal of nuclear materials

www.elsevier.com/locate/jnucmat

Methane penetration in DIII-D ELMing H-mode plasmas

W.P. West [a,*], C.J. Lasnier [b], D.G. Whyte [c], R.C. Isler [d], T.E. Evans [a], G.L. Jackson [a], D. Rudakov [c], M.R. Wade [d], J. Strachan [e]

[a] *General Atomics, P.O. Box 85608, San Diego, CA 92186-5608, USA*
[b] *Lawrence Livermore National Laboratory, P.O. Box 808, Livermore, CA 94551, USA*
[c] *University of California, San Diego, 9500 Gilman Drive, La Jolla, CA 92093-0417, USA*
[d] *Oak Ridge National Laboratory, P.O. Box 2008, Oak Ridge, TN 37831, USA*
[e] *Princeton Plasma Physics Laboratory, P.O. Box 451, Princeton, NJ 08543-0451, USA*

Abstract

Carbon penetration into the core plasma during midplane and divertor methane puffing has been measured for DIII-D ELMing H-mode plasmas. The methane puffs are adjusted to a measurable signal, but global plasma parameters are only weakly affected (line average density, $\langle n_e \rangle$ increases by <10%, energy confinement time, τ_E, drops by <10%). The total carbon content is derived from C^{6+} density profiles in the core measured as a function of time using charge exchange recombination spectroscopy. The methane penetration factor is defined as the difference in the core content with the puff on and puff off, divided by the carbon confinement time and the methane puffing rate. In ELMing H-mode discharges with ion ∇B drift direction into the X-point, increasing the line averaged density from 5 to 8×10^{19} m^{-3} dropped the penetration factor from 6.6% to 4.6% for main chamber puffing. The penetration factor for divertor puffing was below the detection limit (<1%). Changing the ion ∇B drift to away from the X-point decreased the penteration factor by more than a factor of five for main chamber puffing.

PACS: 52.40.Hf; 52.25.Vy
Keywords: Tokamak impurity sources; Carbon contamination; Impurity transport; Chemical sputtering

1. Experiment

The plasma facing surfaces on DIII-D are dominantly graphite and carbon is the dominant impurity in DIII-D during ELMing H-mode operation. The location of the primary source of core carbon contamination has not been clearly identified. As a part of the effort to identify the primary sources of the carbon that reach the core plasma, methane puffing has been carried out to supplement extensive spectroscopic measurements of neutral and molecular carbon [1].

The experiment was carried out in upper single-null. A flux plot is shown in (Fig. 1). Methane was puffed from three locations: (1) the outboard side between the midplane and the X-point, Fig. 1 GASD, (2) into the outer leg of the divertor from the private flux side, PFX1, and (3) the inner wall, GASIW. To control the density in these ELMing H-mode discharges, D_2 was puffed from the outboard side (GASA) and was exhausted using the upper divertor cryopumps. Data will be shown from four discharges: 109296 and 109304, with the ion ∇B drift direction up and $\bar{n}_e = 5 \times 10^{19}$ m^{-3} and 109306, with ∇B drift direction up and $\bar{n}_e = 8 \times 10^{19}$ m^{-3}, and 110454 with the ion ∇B drift direction down and a $\bar{n}_e = 5 \times 10^{19}$ m^{-3}. The GASD valve is fast acting with a direct view of the vacuum vessel. The effective rise and fall times are a few milliseconds. The PFX1 and GASIW valves are connected to their respective puffing zones by long capillary tubes, and have rise and fall times the order of 100 ms.

* Corresponding author. Tel.: +1-858 455 2863; fax: +1-858 455 3569/4156.
E-mail address: west@fusion.gat.com (W.P. West).

0022-3115/03/$ - see front matter
PII: S0022-3115(02)01517-9

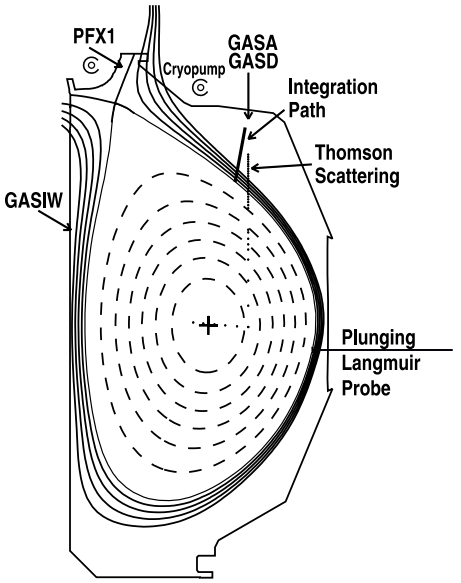

Fig. 1. A cross-section of the DIII-D vacuum vessel is shown along with a flux plot from discharge 109296 at 3100 ms. The locations of the gas puffing valves used for the methane puffing experiments, of the Thomson scattering channels and of the plunging Langmuir probe are also shown. GASA and GASD are at different toroidal locations. The line labeled as integration path in the upper outer SOL is the chord used in the 1-D attenuation model discussed in Section 3.

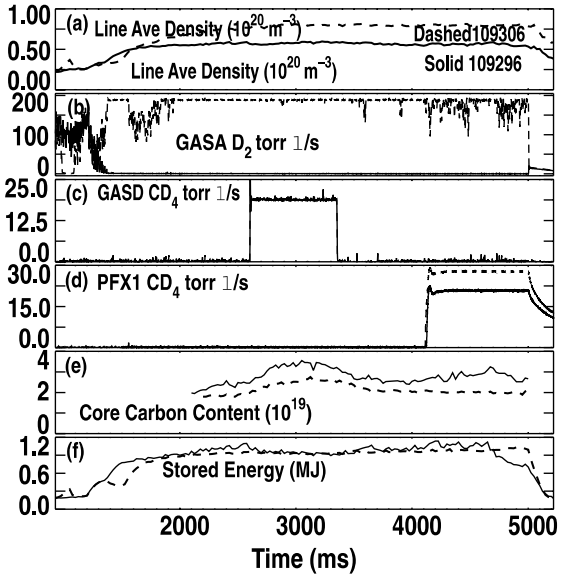

Fig. 2. Time traces of various measured plasma parameters are shown for discharges 109296 (black) and 109306 (dashed).

Selected time traces are shown in Fig. 2. The plasma current is ramped to a flat top of 1.3 MA at 1300 ms. From 1400 ms until the end of flat top at 5000 ms, injected beam power is fixed at 5.5 MW. The discharges transition into H-mode before 1800 ms. Type 1 ELMs begin shortly thereafter and continue throughout the flat top. Line averaged electron density (Fig. 2(a)) is increasing after the L–H transition, but in both discharges it reaches a stable level by 3000 ms. In discharge 109296, a stable operating density of 5.6×10^{19} m^{-3} is maintained with no additional D_2 gas puffing, but to maintain the higher density of 8×10^{19} m^{-3} in 109306 a 190 Torr ℓ/s puff is required (Fig. 2(b)). In both discharges a methane (CD_4) puff from GASD (Fig. 2(c)) is initiated at 2600, and at 3350 ms, after the discharge has reached stable operation, the CD_4 puff is turned off. The total C^{6+} content of the plasma (Fig. 2(e)), determined from charge exchange recombination spectroscopy (CER) [2,3], increases with the CD_4 puff and then decays when the puff is turned off. After the carbon content has decayed from the GASD puff, a second CD_4 puff from the PFX1 valve is initiated at 4100 ms (Fig. 2(d)) and continues until the end of flat top. The plasma stored energy (Fig. 2(f)) is reasonably constant, with an $H_{ITER89P}$ confinement scaling factor of 2.

2. Penetration factor

The penetration factor, P_f, is defined as the ratio of the source of carbon inside the separatrix to the throughput of methane from the gas valve. The throughput for each gas valve is calibrated off line and is accurate to $\pm 5\%$. Since the plasma has reached a steady condition by the end of the methane puff, the source of carbon in the core must equal the outflow of carbon from the core. The outflow is determined from the change in the total C^{6+} content of the plasma in the core due to the puff divided by the confinement time of C^{6+}. The total carbon content is obtained from the C^{6+} density profiles measured by CER and integrated over the volume of the plasma. The C^{6+} confinement time, the initial value of C^{6+} content and the background level of C^{6+} from the intrinsic sources are obtained from an exponential fit to the decay of the core C^{6+} content after the GASD methane puff is stopped. The time behavior of the core C^{6+} content for three discharges with GASD and PFX1 methane puffs is shown in Fig. 3 along with exponential fits to the decay phase.

$$N^{C^{6+}}(t) = N^{C^{6+}}_{puff} e^{-(t-t_0)/\tau_C} + N^{intr}, \quad (1)$$

where $N^{C^{6+}}_{puff}$ is the core carbon content from the puff, τ_C is the decay time, and N^{intr} is the offset due to intrinsic carbon. The core carbon source due to the puff is given by $N^{C^{6+}}_{puff}/\tau_C$.

Table 1 gives the results of the measured carbon confinement time, energy confinement time and P_f for

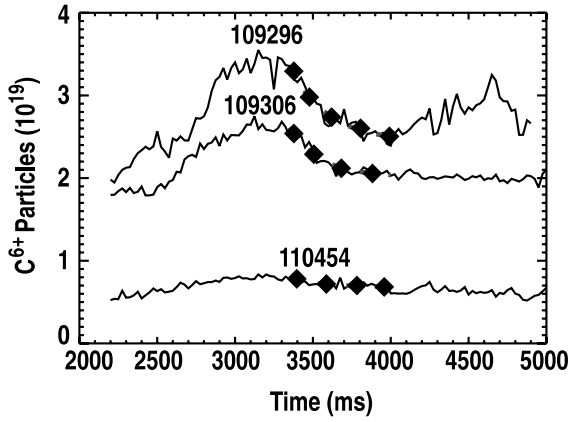

Fig. 3. The total core C^{6+} content is shown as a function of time for three discharges, 109296, 109306, and 110454 along with the exponential fits (diamonds) to the decay phase after the GASD valve is turned off. The time duration for the GASD and PFX1 valves is shown by the horizontal bars.

the three outer wall puff discharges. Comparison of the results on the outer wall puff from the two discharges with ion $B \times \nabla B$ drift direction toward the X-point, 109296 and 109306, shows that the increase in the line average density (Greenwald factor from 0.5 to 0.7) decreased the penetration factor by only 30%.

From Table 1 we see that the inner wall puff had a larger P_f than the outer wall puff. Since the inner wall puffing valve has a relatively slow response time, the GASIW puff (discharge 109304) is held on sufficiently long that the gas throughput and the plasma response have both reached an equilibrium state. The change in carbon content due to the puff is taken as the increase in the total carbon content from the pre-puff level, and the carbon confinement time is assumed to be the same as measured in discharge 109296. Analysis of the divertor puff (PFX1) is problematic. In discharge 109296 there is an apparent increase in the carbon content due to the PFX1 puff. However in the other two discharges 109306 and 110454 (and in discharges not shown here) the divertor puff had little affect on the core carbon. After 4000 ms in discharges 109296 (during the divertor region puff) and 109304 (during the inner wall puff) the plasma stored energy climbs slightly and the discharges show signs of encountering MHD instabilities. This MHD activity is more likely to be the cause of the increase in the carbon content at the end of discharge 109296 than the methane puff. Considering all the available data, we have determined that the divertor P_f is below the limit of measurability (<1%). The increase in core carbon after 4000 ms in discharge 109296 is small compared to that in 109304 and introduces only a small error in the measurement of inner wall penetration.

The most dramatic change in P_f occurs due to a change in toroidal field direction. When the ion $B \times \nabla B$ drift direction is down (away from the X-point), the core carbon concentration is much lower both during and after the CD_4 puff. As seen in Table 1 for discharge 110454, P_f is also much lower, more than a factor of five below the comparable discharge with the ion ∇B drift direction up.

3. SOL properties and neutral penetration

The break up of methane and the resulting transport of carbon through the SOL is a complex process. In the far SOL the electron temperature (<10 eV) is below or near the threshold for ionization and dissociation processes with ground state methane. The ion temperatures are high, the order of 100 eV, leading to fast charge exchange with deuterons [4]. At these low electron temperatures the dissociative recombination process with CD_4^+ is fast, producing neutral radicals. This charge exchange/dissociative recombination process will likely cascade through the CD_y radicals, leading to the production of neutral carbon flux at about 1 eV temperature. In DIII-D a carbon neutral temperature of 1 eV is measured spectroscopically under conditions where chemical sputtering is expected to dominate over physical sputtering [1]. The neutral carbon that penetrates to the core from the methane puff is most likely due to the 1 eV carbon produced in the SOL from the stepwise dissociation of CD_4. SOL profiles of n_e and T_e are obtained from Thomson scattering and a plunging Langmuir probe. The results of a 1-D model for attenuation

Table 1
The parameters obtained from fitting the decay phase of the core carbon content and the calculated carbon penetration factor

Discharge	Gas valve	Puff rate (10^{20} s^{-1})	τ (carbon) (ms)	τ_E (ms)	n_e (10^{19} m^{-3})	N^{C6+}_{puff} (10^{19})	N^{intr} (10^{19})	P_f (%)
109296	GASD	6.6	157	165	5.6	0.7	2.5	6.6
109304	GASIW	6.9	157[a]	176	5.0	1.1	3.8	10.1
109306	GASD	6.6	197	163	8.2	0.6	2.0	4.6
110454	GASD	6.5	167	168	5.0	0.12	0.7	1.1

[a] Taken from discharge 109296.

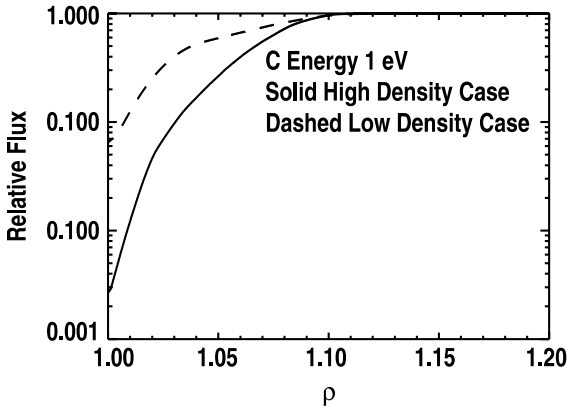

Fig. 4. The modeled attenuation of 1 eV neutral carbon as it penetrates the SOL along the chord shown in Fig. 1 for discharges 109304 and 109306 is shown.

of an inward flux of 1 eV neutral carbon originating at $\rho = 1.2$ are shown in Fig. 4, considering only electron impact ionization [5]. The charge exchange rate for deuterons onto neutral carbon is relatively weak [6]. The 1-D path chosen for the calculation shown in Fig. 4 goes through the SOL along a chord passing from the GASD valve through the magnetic axis of the plasma (see Fig. 1). For the lower line averaged density case, about 6.5% of the original carbon flux from the edge reaches the separatrix, in reasonable agreement with the measurement of 6.6% considering the crudeness of the model. However, in the higher line averaged density case the SOL electron density is almost three times higher while the SOL electron temperature remains about the same. The result is the calculated neutral carbon penetration is only about 0.26% while the measured value is 4.6%. The SOL electron density and temperature profiles for the ∇B down case are not significantly different from the ∇B up case at comparable line averaged density.

4. Main chamber carbon source from chemical sputtering

We can use the measured penetration factors to get a rough estimate of core contamination due to chemical sputtering at the main chamber wall. An estimate of the wall flux of methane into the SOL at the midplane can be obtained from a spectroscopic measurement of the intensity of the CD emission band at 4305 Å. After correcting for geometric factors, the band intensity can be converted to the methane flux, Γ_{CD_4}, using the measured photon production efficiencies of 100 CD_4 molecules/photon at typical SOL electron temperatures [7,8]. Assuming poloidal uniformity, the core carbon content, N_C, is then given by

$$N_C = \Gamma_{CD_4} P_f A_{sep} \tau_C, \quad (2)$$

where A_{sep} is the surface area of the last closed flux surface. The fraction of core carbon is given by N_C/N_e, where N_e is the total electron content of the plasma. In discharge 109296, the low density case, the SOL emissivity of the CD band is measured to be 2×10^{18} ph/m^2/s resulting in a methane influx of about 1×10^{20} m^{-2} s^{-1}. From Eq. (2) we obtain a core carbon fraction of 1–5%. A range is quoted due to uncertainty in geometric corrections and poloidal uniformity. The measured core carbon fraction is 3%, indicating that main chamber chemical sputtering is playing a significant role in core contamination.

5. Discussion

In the limited density scan reported here penetration of carbon into the core plasma decreases only slightly as the line averaged density was increased from 5×10^{19} to 8×10^{19} m^{-3} even though the SOL density and opacity to neutral C increased much more. The ansatz of SOL shielding by neutral ionization seems to be too simple. Carbon content in the core plasma is controlled not only by the carbon source inside the separatrix, but also by the carbon density at the separatrix, i.e. the boundary condition presented by the wall source and the SOL impurity transport. SOL transport of carbon ions, which sets the carbon density boundary condition for the core, may be more important in determining core carbon content than penetration of neutrals. Changing the direction of the toroidal magnetic field, which changes both the $B \times \nabla B$ and $E \times B$ drift directions, made a very large change in the core carbon content due to both intrinsic and puffed sources of carbon. This fact suggests that drifts are important in SOL impurity transport. The fact that drifts play an important role in SOL impurity transport has been shown previously [9]. Achieving a detailed predictive capability of core impurity contamination will require coupling of edge plasma transport models that include drifts to core transport models. Penetrations factors, combined with spectroscopic measurement of the SOL CD emission, indicate that main chamber chemical sputtering is an important contributor to carbon contamination of the core plasma.

Acknowledgements

Work supported by US Department of Energy under Contracts DE-AC03-99ER54463, W-7405-ENG-48, DE-AC05-00OR22725, DE-AC02-76CH03073, and Grant DE-FG03-95ER54294.

References

[1] R.C. Isler, R.J. Colchin, N.H. Brooks, T.E. Evans, W.P. West, D.G. Whyte, Phys. Plasmas 8 (2001) 4470.

[2] K.H. Burrell, D.H. Kaplan, P. Gohil, D.G. Nilson, R.J. Groebner, D.M. Thomas, Rev. Sci. Instrum. 72 (2001) 1028.
[3] M.R. Wade, W.A. Houlberg, L.R. Baylor, Phys. Rev. Lett. 84 (2000) 282.
[4] R.K. Janev, D. Reiter, Report FZJul., 2002, p. 3966.
[5] H.P. Summers, ADAS, Atomic Data and Analysis Structure, Originally developed by the Jet Joint Undertaking, 1st Addition User Manual, 1994.
[6] P.C. Stancil, J.-P. Gu, C.C. Havener, P.S. Kristic, D.R. Schults, et al., J. Phys. B: At. Mol. Opt. Phys. 31 (1998) 3647.
[7] M.F. Stamp, S.K. Erents, W. Fundamenski, G.F. Matthews, R.D. Monk, J. Nucl. Mater. 290–292 (2001) 321.
[8] D. Naujoks, D. Coster, H. Kastelewicz, R. Schneider, J. Nucl. Mater. 266–269 (1999) 360.
[9] S. Gangadhara, B. LaBombard, C. MacLatchy, J. Nucl. Mater. 290–293 (2001) 598.